ENERGY STORED AND DISSIPATED IN SKELETAL MUSCLE BASEMENT MEMBRANES DURING SINUSOIDAL OSCILLATIONS

JAMES G. TIDBALL
Division of Biomedical Sciences, University of California, Riverside, California 92521

ABSTRACT We subjected single skeletal muscle cells from frog semitendinosus to sinusoidal oscillations that simulated the strain experienced as the cells near the end of passive extension and begin active contraction in slow swimming. Other cells from which the basement membrane was removed by enzymatic and mechanical procedures were tested identically. Effectiveness of the basement membrane removal technique was evaluated by electron microscopy, by an electrophoretic and lectin-binding assay for depletion of cell surface glycoproteins, and by confirmation by means of electrophoretic and immunologic analyses that major intracellular, cytoskeletal proteins were not disrupted. Measurements of maximum stress, maximum strain, and phase lag between these maxima enabled the complex modulus (dynamic stiffness) and loss tangent (relative viscous losses to elastic energy storage) to be calculated for each mechanically tested preparation. We also calculated the amounts of energy stored and dissipated in each preparation. These calculations indicate that cells with intact basement membranes have complex moduli significantly greater than those of cells without basement membranes, and that cells with basement membrane store significantly more elastic energy than basement membrane depleted cells. However, when subjected to identical sinusoidal strains, energy dissipation in cells with intact basement membranes is over three times greater than dissipation in cells without basement membrane. The relative magnitudes of energy losses to energy storage, called the specific loss, is nearly three times greater for intact cells than for basement membrane depleted cells. Basement membranes may thereby serve as a brake for slowing passive extension of muscle before contraction begins.

INTRODUCTION

Basement membranes have been shown to have specialized functions in various tissues. In addition to supporting parenchymal cells, basement membranes may act as a filter for solutes (e.g., see reviews by Kefalides et al., 1979; Heathcoat and Grant, 1981; Farquhar, 1982), may influence cell development and differentiation (e.g., Hay, 1978, 1982; Van Exan and Hall, 1983) and serve as a substratum for cell migration (e.g., for discussion, see Bernfield and Bannerjee, 1978; Sanders, 1983).

This study concerns the role of skeletal muscle basement membranes in the energetics of locomotion. In particular, the stage of locomotion evaluated is that in which passively extended muscle reaches the end of extension and begins active contraction. The range of sarcomere lengths at which this occurs was determined in an earlier study (Tidball and Daniel, 1986). During this stage of locomotion, muscle stores mechanical energy as reversible deformations of structural molecules. The energy thus stored is released when active contraction begins, and this energy adds to the total power output of the muscle (Tidball and Daniel, 1986). Elastically stored energy in muscle can make substantial contributions to the efficiency of locomotion (e.g., see Cavagna et al., 1964; Cavagna et al., 1977). A previous study (Tidball and Daniel, 1986) postulated that basement membranes may be a site of energy storage during locomotion. That hypothesis is tested here by comparing energy storage capabilities of control muscle cells to those from which the basement membrane has been removed. Those parameters are then used to calculate the energy stored in basement membranes that contributes to force generation during active muscular contraction and the energy dissipated in basement membranes during this same stage of locomotion.

The effectiveness of the basement membrane removal technique used in the present study is evaluated by: (*a*) electron microscopic examination to establish that the basement membrane is removed and (*b*) by determining that the only muscle proteins which appear depleted in electrophoretic separations are those that are partially or wholly extracellular. The integrity of intracellular proteins is assayed in cells from which basement membranes have been removed by: (*a*) confirming that the cells are still contractile, (*b*) establishing that the relative molar ratio of major intracellular, structural proteins is unperturbed, and (*c*) investigating the ultrastructural appearance of the cell after basement membrane removal.

MATERIALS AND METHODS

Removal of Basement Membranes

Adult frogs (*Rana pipiens*, either sex) were pithed and their semitendinosus muscles exposed by dissection. Each semitendinosus muscle was tied to an applicator stick and immersed in either (*a*) 75 mM potassium acetate, 5 mM magnesium acetate, 5 mM K_2 ethylene-glycol-bis(β-aminoethyl-ether)-*N*,*N*'-tetraacetic acid, and 2% povidone (molecular weight = 40,000) in 15 mM sodium phosphate buffer at pH 7.0 (solution A, Magid and Reedy, 1980) or (*b*) 130 mM sodium chloride, 4 mM potassium chloride, 1 mM magnesium chloride, 1 mM sodium carbonate, 0.5 mM sodium phosphate, 5.6 mM glucose, 0.25 mM calcium chloride, 0.4 mM adenosine triphosphate, 0.1% collagenase (Type IV [Sigma Chemical Co., St. Louis, MO]) and 0.2% hyaluronidase (Type V [Sigma Chemical Co.]) at pH 7.2 (solution B, Brady et al., 1979). The muscles were maintained in these solutions for 30 min at 25°C and then transferred to fresh solution A. Those muscles treated with solution A only are called controls; those treated with solution B are called enzyme-treated. The collagenase used in this study will cause proteolysis of myosin (Sigma Chemical Co., technical information), but no evidence of thick filament disruption was obtained either from mechanical data or electron microscopic study of solution B–treated cells. This indicates that the cell membranes were intact throughout treatment with solution B.

Single skeletal muscle cells were dissected from the surface of both enzyme-treated and control muscles. Care was taken to use only those cells lying at a muscle's surface because deeper cells presumably were not exposed to the same concentration of solutes during the 30-min incubation.

Mechanical Testing

Cell Dissections. Single skeletal muscle cells were dissected free from frog semitendinosus by using fine needles to remove the epimysium and separate individual cells from their neighbors. The cells that were used showed no apparent disruptions in their structure when viewed through the dissecting microscope. The cells were also examined by electron microscopy at the end of mechanical testing to further check their structural integrity. Data gathered from those cells showing disruptions in myofibril structure as observed by electron microscopy were rejected. All dissections and mechanical testing were performed in rigor solution A at room temperature (21–23°C). Solution A was chosen for control cells, since x-ray diffraction studies have shown that immersion of permeabilized frog muscle cells in this solution could give patterns "almost indistinguishable from living muscle" (Magid and Reedy, 1980) and single cell dissections produce tears in the cell membrane which allow solution A access to intracellular spaces.

Cells were placed in rigor before testing to maximize the number of actomyosin crossbridges present. This was done because muscle actively forms crossbridges at the final stage of passive extension before active shortening begins (Asmussen and Bonde-Petersen, 1974; Marsden et al., 1983) and the present study was directed toward investigating muscle behavior at that stage.

Testing Apparatus. Periodic stress-strain measurements were carried out at 1 Hz on a low-frequency, forced vibration instrument constructed in collaboration with Dr. Thomas L. Daniel (University of Washington, Seattle). For testing in this apparatus (Fig. 1), each cell was clamped between two stainless steel wire clamps. One wire clamp was attached directly to a pen-motor drive from a chart recorder (Texas Instruments Oscillowriter, Houston, TX). Sinusoidal strains to be placed on a specimen were generated by the pen motor. The frequency and amplitude of the pen's vibration were set by a waveform generator (model 3311A, Hewlett-Packard, Sunnyvale, CA). The other clamp was welded to a force platform that consists of a thin piece of stainless steel shim stock

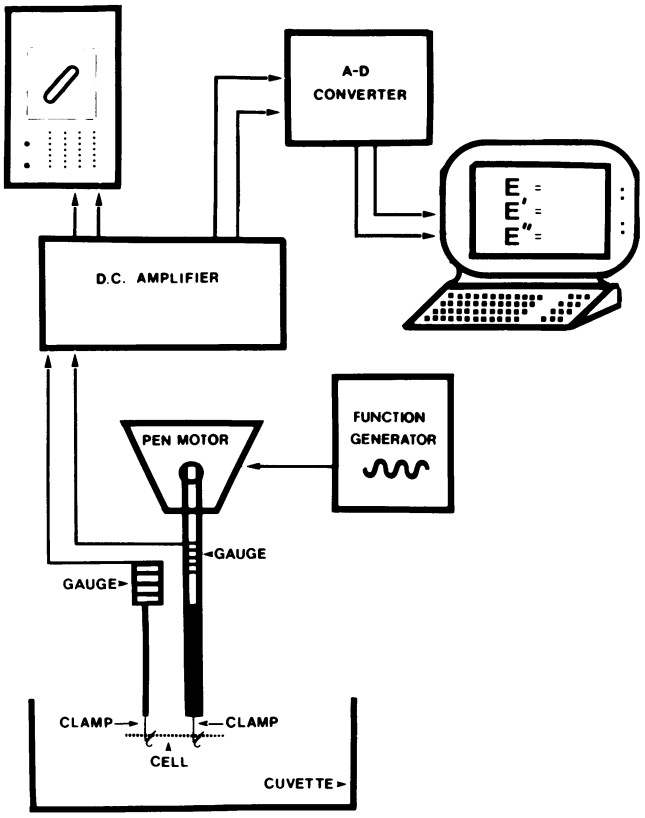

FIGURE 1 Schematic diagram of muscle-testing apparatus. Selected waveform is generated (waveform generator) to drive pen motor, which forcibly oscillates one end of a clamped cell. The cell is clamped between the folds of a bent, stainless-steel wire. The movements of the driving arm are monitored by a strain gauge, the deflections of which are used to monitor cell strain. The other clamped end of the cell also oscillates in response to forced oscillation. The movements of this end of the cell are also monitored by a strain gauge. Changes in resistance across the deformed strain gauge result in changes in current. This direct current across the gauges are amplified (D.C. amplifier). Associated changes in voltage are displayed as analog data on an oscilloscope screen with strain as a function of force. The analog data are also converted to digital data and analyzed on line using an IBM-PC.

equipped with a strain gauge. The force platform was calibrated with known weights and had a maximum sensitivity of about 10 dynes.

Deformations of the cells were monitored by recording the change in clamp-to-clamp distance. A strain gauge was attached to the drive portion of the pen motor and the gauge's deflection was used to measure imposed deformations on the cell. The driving clamp was supported by a 1 cm thick piece of plexiglass, so there was no deformation of the driving clamp at these forces. Corrections were made for the movements of the second clamp that was mounted at the opposite end of the preparations. Deflections of both clamps were monitored continuously throughout testing. Thus, total deformation (ΔL) was the movement of the driving clamp minus that of the second clamp.

Initial length and width of each specimen were measured with an ocular micrometer to determine stress (σ = force/area) and strain ($\epsilon = \Delta L/L_o$) where ΔL is the deformation (change in length) and L_o is the initial length.

Cell strains were also measured by recording the sarcomere length of the cell before loading (L_s) and the increase in sarcomere length while loaded (ΔL_s). This was done by measuring changes in diffraction spacings obtained from a laser beam (model 155 He-Ne laser, SpectraPhysics,

Mountain View, CA) passed through the cell and reflected off a mirror onto a calibrated screen. Cell strain was equivalent to $\Delta L_s/L_s$.

Signals from the force platform and the strain monitor attached to the pen motor were amplified with a two-channel bridge amplifier. The force applied to a cell and the resulting strain were recorded on an X-Y oscilloscope. The amplified signals were presented on the screen of the oscilloscope as Lissajous figures. The Lissajous figures provided a quick visual check of the performance of the preparation.

The amplified, analog signals were also transmitted to an IBM personal computer equipped with an analog to digital conversion board (board DT2805; Data Translation, Marlborough, MA). Data were collected and digitized at 13 kHz. The stored data were then evaluated to determine the maximum imposed strain placed on the preparation, the maximum stress during the same cycle of loading, and the time lag between the two maxima. Those data yielded through the calculations outlined below moduli that express the amount of applied energy that was stored in the cell as reversible deformations (the storage modulus), the amount of applied energy that was lost as heat or in plastic deformations (the loss modulus), and the damping in the system (the ratio of loss to storage moduli).

The loading device can resolve movements of <80 μm. Preparations used for loading were typically >1-cm long. Therefore, strain measurements were accurate enough to resolve length changes of <0.8%.

Changes in force of 10 dynes (10^{-4} N) could be resolved with the force platform. Calculations (Tidball, 1983) based on the measurements of others (Ramsey and Street, 1940) show that single twitch muscle cells generate a maximum isometric stress of $\sim 3 \times 10^5$ N $\cdot$ m^{-2}. This stress represents a force of 2×10^{-3} N for a typical cell 80 μm in diameter. The loading device was capable of resolution 20 times greater than that needed to record the force of a single cell twitch.

Slippage of the specimens at the clamps was evaluated by mounting a single muscle cell in the loading device and passively extending the cell using stresses larger than those used in the experimental protocol. Strain of the cell was measured both by recording changes in sarcomere length optically and simultaneously recording changes in clamp-to-clamp distance. Strain measurements recorded by both techniques agreed. Since at no time did sarcomere length decrease while clamp-to-clamp distance increased, it was concluded that no measurable slippage occurs at the clamp.

We investigated the structural effects of clamping by electron microscopy. The myofibrils at clamping sites were found in disarray yet undivided and therefore still in mechanical continuity with those in the unclamped regions of the cell.

Data Analysis

For a cell subjected to sinusoidal, forced loading, the strain at any chosen time $\epsilon(t)$ is a function of the maximum strain (ϵ_o) corrected for the sinusoidal waveform where ω is the circular frequency and t is time:

$$\epsilon(t) = \epsilon_o \sin \omega t. \tag{1}$$

Viscoelastic materials that are sinusoidally loaded experience sinusoidal stresses; yet the maximum stress occurs at some time other than the time of maximum strain (Ferry, 1970). The time lag or phase lag (δ) between these maxima increases as the relative importance of viscosity to elasticity increases in the determination of the material's behavior (Ferry, 1970). The stress at any time $\sigma(t)$ varies sinusoidally with the maximum stress (σ_o) corrected for the waveform and the phase lag.

$$\sigma(t) = \sigma_o \sin (\omega t + \delta). \tag{2}$$

The relationship between maximum stress and maximum, associated strain for the cell is expressed by a complex modulus, E^*.

$$E^* = \sigma_o/\epsilon_o, \tag{3}$$

so that, through Eqs. 1–3,

$$E^* = [\sigma(t)/\sin (\omega t + \delta)][\sin (\omega t)/\epsilon(t)]. \tag{4}$$

Solving for $\sigma(t)$, we get

$$\sigma(t) = [E^* \epsilon(t) \sin (\omega t + \delta)] [\sin (\omega t)]^{-1}. \tag{5}$$

Combining Eqs. 1 and 5 we get,

$$\sigma(t) = [E^* \epsilon_o \sin (\omega t) \sin (\omega t + \delta)][\sin (\omega t)]^{-1}. \tag{6}$$

Simplifying this, we have

$$\sigma(t) = E^* \epsilon_o \sin (\omega t + \delta). \tag{7}$$

Eq. 7 is expanded to give

$$\sigma(t) = \epsilon_o(E^* \cos \delta) \sin \omega t + \epsilon_o(E^* \sin \delta) \cos \omega t. \tag{8}$$

Eq. 8 is used to define two additional parameters:

$$E' = E^* \cos \delta, \tag{9}$$

$$E'' = E^* \sin \delta, \tag{10}$$

where E'' (the loss modulus) is a measure of the viscous energy loss per cycle of oscillation or the out-of-phase component of loading. E' (the storage modulus) is a measure of the energy stored and returned without loss in each cycle of oscillation. The ratio E''/E' is defined as the damping and is equal to tan δ (Ferry, 1970).

Measurements of the stress, maximum strain, frequency of oscillation, and the phase angle with the use of Eq. 7 provide a means to calculate the complex modulus of a material. The storage and loss moduli are calculated from the complex modulus according to Eqs. 9 and 10.

Energy Storage in Muscle Cells

The ratio of energy stored to energy lost in each cycle of sinusoidal loading is proportional to tan δ (Ferry, 1970). The average energy stored per unit volume of a cell in each cycle of sinusoidal loading is ξ_s (Ferry, 1970) where

$$\xi_s = \int_0^{\epsilon_o} E' \epsilon(t)\, d\epsilon(t), \tag{11}$$

which, through integration, yields

$$\xi_s = E' \epsilon_o^2/4, \tag{12}$$

where $\epsilon(t) = \epsilon_o \sin \omega t$.

The average energy loss per unit volume of a cell in each cycle of sinusoidal loading is ξ_d (Ferry, 1970) where

$$\xi_d = \pi \epsilon_o \sigma_o \sin \delta. \tag{13}$$

Substitution, using Eq. 3, yields

$$\xi_d = \pi \epsilon_o^2 E^* \sin \delta. \tag{14}$$

Substituting Eq. 10 yields

$$\xi_d = \pi \epsilon_o^2 E''. \tag{15}$$

The specific loss of energy in each cycle of loading is defined as one half the ratio of energy dissipated to energy stored (Ferry, 1970). Thus,

$$\tfrac{1}{2}(\xi_d/\xi_s) = 2\pi \tan \delta \tag{16}$$

Electrophoresis, Gel Staining, and Lectin Binding

Glycoproteins, including Type IV collagen and laminin, comprise a major portion of basement membranes and bind wheat germ agglutinin (WGA) (Foidart et al., 1982). Control and enzyme-treated muscle were evaluated for WGA-binding to determine whether WGA-binding proteins were removed in the enzymatic treatment.

Strips of muscle were removed from the surface of control and enzyme-treated muscle and homogenized in 10 vol of 50 mM Tris buffer at pH 7.5 containing 150 mM sodium chloride and 0.1% sodium azide (buffer A). The muscle samples were then boiled in buffer A containing sodium dodecyl sulfate (SDS) and centrifuged to remove any large, unsolubilized muscle fragments. The samples were then electrophoresed on SDS polyacrylamide gels electrophoresis (PAGE), which contained 12% acrylamide and 0.13% bisacrylamide (Laemmli, 1970). Molecular weight markers were run in parallel lanes (myosin [200 kD]; phosphorylase [95 kD]; bovine serum albumin [68 kD]; ovalbumin [45 kD]). Some gels were stained with Coomassie Blue and other, identical gels were stained by the periodic acid-Schiff (PAS) technique (Allen et al., 1984). Gels loaded identically to those stained with Coomassie Blue and PAS were electrophoretically transferred to nitrocellulose sheets (Burnette, 1981). Some transfers were made at 0.5 amps for 1 h; others were made at 0.1 amps for 13 h followed by 0.5 amps for 0.5 h. The nitrocellulose was then washed at 4°C for 0.5 to 2 d in buffer A containing 0.2% gelatin and 0.05% Tween-20. The sheets were then incubated at room temperature with ^{125}I-WGA agglutinin (New England Nuclear, Boston, MA) for 1.5 h and then rinsed six times for 30 mins in buffer A containing 0.2% gelatin and 0.05% Tween-20, air dried and autoradiographed.

Coomassie blue stained gels of control and enzyme-treated muscles were compared by scanning densitometry (Hoeffer GS-300 densitometer equipped with a Sargent-Welch SRG-2 recorder and electronic integrator). Peak areas were used to calculate relative molar ratios of known skeletal muscle proteins. This assay was used to determine whether the enzymatic treatment disrupted any major, intracellular, cytoskeletal proteins.

Immunolabeling

Alpha-actinin is a major cytoskeletal protein of skeletal muscle. To be able to determine whether the enzymatic treatment disrupted its molar ratio relative to other major cytoskeletal proteins, the relative molecular weight of α-actinin in one dimensional electrophoretic separations was established in immunoblotting procedures.

Muscle samples were separated by one dimensional gels and transferred to nitrocellulose as described above. The nitrocellulose sheets were washed in buffer A containing 3% bovine serum albumin, 0.2% gelatin, and 0.05% Tween-20 for 4 h to overnight at room temperature. The nitrocellulose was then incubated for 90 min at room temperature in anti-α-actinin diluted 1:500 in 0.2% gelatin 0.05% Tween-20, 5% vol/vol inactivated horse serum in buffer A. The anti-serum, a gift from Dr. Keith Burridge, University of North Carolina, Chapel Hill, was manufactured in rabbits against chicken smooth muscle α-actinin. The nitrocellulose sheets were washed extensively in 0.2% gelatin, 0.05% Tween-20 in buffer A and then incubated for 1 h at room temperature in ^{125}I-

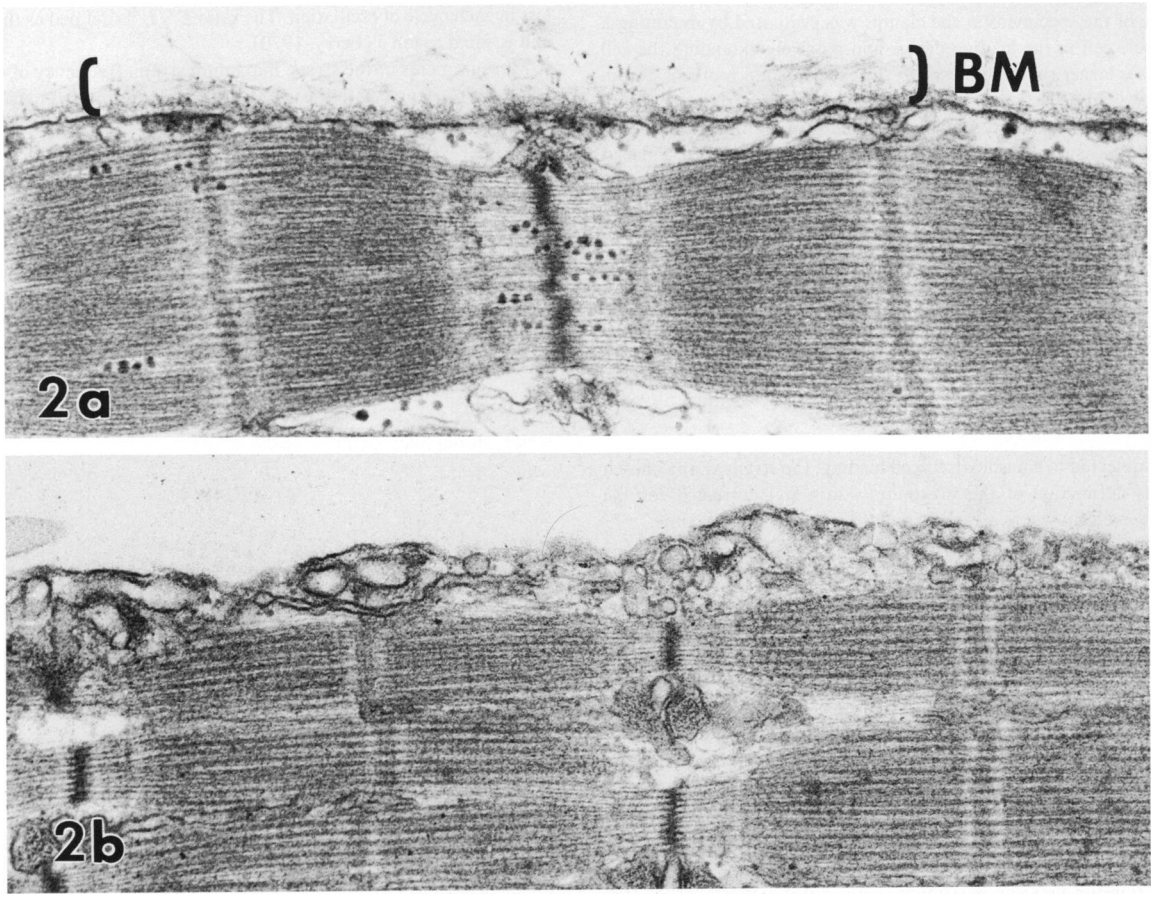

FIGURE 2 (*a*) Longitudinal section through single dissected skeletal muscle cell. This is a control cell around which there is an intact basement membrane (*BM*). ×38,000. (*b*) Longitudinal section through single dissected skeletal muscle cell. This cell was from a muscle treated with collagenase and hyaluronidase before single cell dissection. ×38,000.

affinity-purified, goat anti–rabbit IgG. This antibody was iodinated using the chloramine T method (Hunter and Greenwood, 1962). The sheets were incubated in a solution containing 10^6 cpm/ml ^{125}I and 2% hemoglobin, 0.2% gelatin, 0.05% Tween-20 in buffer A and then washed, air dried, and exposed for autoradiography.

Electron Microscopy

Each cell was fixed at the end of mechanical testing by immersion in 1.4% glutaraldehyde in 0.1 M sodium cacodylate with 4 mM $CaCl_2$ at pH 7.2 for 15 min. The cells were then rinsed in cacodylate buffer, removed from the testing device and fixed in 1% osmium tetroxide for 10 mins. The cells were then ethanol dehydrated and embedded in epoxy resin. Longitudinal sections were cut at ~60 nm thickness and viewed in a Siemens 101 electron microscope. Cells were evaluated to determine whether they suffered obvious structural damage during preparation and testing, in which case the data were discarded. Maximum and minimum basement membrane thicknesses were measured for each cell used for analysis.

RESULTS

Evaluation of Enzymatic Treatment

Electron microscopic analysis of single, control cells showed that these cells are ensheathed by a basement membrane that may vary in thickness from 100 to 300 nm along the length of any one cell (Fig. 2). Electron microscope studies of single, enzyme-treated skeletal muscle cells showed that the enzymatic treatment described here is adequate to disrupt the basement membrane and associated connective tissue surrounding the cells (Fig. 2). No electron microscopic evidence of disruption or extraction of intracellular, cytoskeletal structures was observed, although some tearing of the plasma membrane was recorded. Similar damage to the plasma membrane was observed in control and enzyme-treated cells that suggests that the single cell dissection procedure rather than enzyme-treatment caused membrane tearing. Cells stimulated after enzyme treatment were still contractile.

SDS PAGE of control and enzyme-treated skeletal muscle and of epimysium and tendon showed that some of the proteins removed or diminished by the enzymatic treatment are of the same molecular weight as proteins that bind ^{125}I-WGA (~58, 38, and 34 kD) (Fig. 3), which indicates that they are partly or entirely extracellular. Those bands that bound WGA also displayed a positive PAS reaction (data not shown). Other proteins whose concentration was diminished by enzymatic treatment (~260, 240, and 44 kD) have the same molecular weight as proteins that are enriched in epimysium or tendon (Fig. 4). The depletion of these proteins during enzymatic treatment and dissection of intact cells indicates that either these proteins are entirely extracellular or that each has an

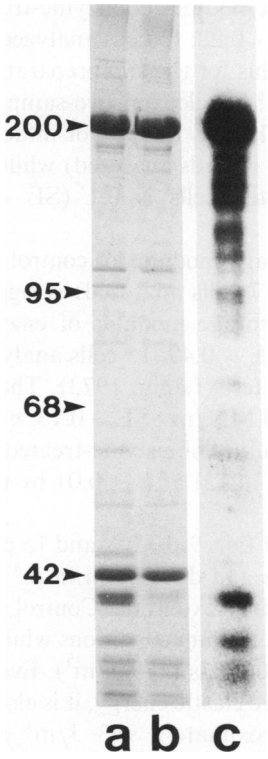

FIGURE 3 Lanes *a* and *b* are photographs of a one-dimensional polyacrylamide gel of control muscle (*a*) and collagenase and hyaluronidase-treated muscle followed by single cell dissection (*b*). The gel is stained with Coomassie Blue. Bands with molecular weights of ~260, 240, 58, 44, 38, and 34 kD are depleted in the enzyme treated muscle. Immunoblots of control muscle treated with ^{125}I-wheat germ agglutinin (*c*) show that there are WGA-binding substances at 58, 38, 34 kD and other locations in the blots.

FIGURE 4 One-dimensional gels of semitendinosus tendon (*a*) and whole, associated, control muscle (*b*). Bands with molecular masses of ~260, 240, and 44 kD correspond in the two preparations.

extracellular domain that was exposed to the enzymatic treatment.

Antisera to chicken gizzard smooth muscle α-actinin applied to immunoblots of frog skeletal muscle bound to a 110-kD frog protein (Fig. 5). This 110-kD band comprises a large portion of the total protein in frog skeletal muscle and has approximately the same molecular weight as the chick protein against which the anti-serum was manufactured. These observations indicate that the 110-kD band in one-dimensional SDS PAGE of frog skeletal muscle is α-actinin (Fig. 5). A previous investigation showed that frog's myosin heavy chain and actin are of the same relative molecular weights as rabbit's myosin heavy chain and actin when estimated by PAGE (Ferenczi et al., 1978). This indicates that the prominent 200- and 42-kD bands seen by PAGE in this study are of myosin and actin, respectively. Another, nonmyosin protein must also lie at circa 200 kD in one-dimensional PAGE to account for this band's WGA-binding behavior. However, this nonmyosin protein is expected to be a proportionately minor component of the 200-kD band, since frog skeletal muscle is >80% myofilaments (vol/vol) (Mobley and Eisenberg, 1975) and myosin is a major constituent of myofilaments.

Quantitative scanning densitometry of control and enzyme-treated muscle shows that the molar ratio of (myosin heavy chain)/(α-actinin)/(actin) was little effected by enzymatic treatment of the muscle. The ratio of (myosin heavy chain)/(α-actinin)/(actin) for control muscle in this preparation is approximately 1.0:0.26:2.7. The same ratio for enzyme-treated muscle is approximately 1.0:0.28:2.7. These data were not corrected for the presence of nonmyosin, WGA-binding protein(s) that are found at ~200 kD in one-dimensional gels.

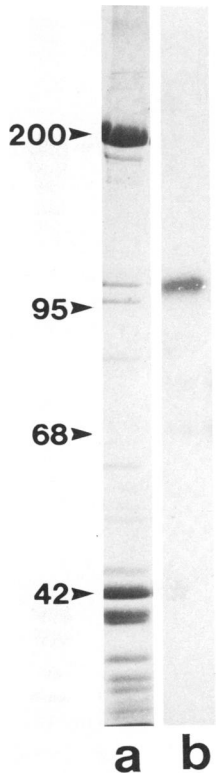

FIGURE 5 One-dimensional gel of control muscle (*a*) stained with Commassie Blue and control muscle transferred to nitrocellulose, incubated with anti-α-actinin followed by ^{125}I-goat anti-rabbit IgG and then autoradiographed (*b*). The α-actinin band is localized to the prominent 110-kD band in frog skeletal muscle.

Mechanical Behavior of Enzyme-treated and Control Cells

Sinusoidal loading of single, control or enzyme-treated cells in the present study showed that enzyme treatment significantly reduces cell stiffness and the loss tangent of cells loaded at strains of 0.7 to 2.7% at sarcomere lengths (L_s) = 2.6–2.8 μm (Table I). A previous study has shown that these sarcomere lengths of 2.6–2.8 μm are those at which passive extension of these cells ends and active contraction begins in locomotion (Tidball and Daniel, 1986). Data collected by numerous investigators indicate that sinusoidal strains of this magnitude are smaller than those required to cause crossbridge slippage (for discussion, see Tidball and Daniel, 1986). The complex modulus of single, control cells loaded under these conditions is 3.29 MN/m^2 (standard error (SE) = 0.40; 17 cells analyzed) while the complex modulus of enzyme-treated cell is E^* = 1.8 MN/m^2 (SE = 0.28; 15 cells analyzed). The difference in complex modulus for the two preparations is significant at $P \leq 0.05$ by the Wilcoxon two-sample, rank-sum test (Lapin, 1973). The loss tangent of intact, control cells is 0.37 (SE = 0.08; 17 cells analyzed) while the loss tangent for enzyme treated cells is 0.1 (SE = 0.05; 15 cells analyzed).

The mean storage modulus of control cells (3.09 MN/m^2; SE = 0.53; 17 cells analyzed) is significantly greater than the mean storage modulus of enzyme-treated cells (1.79 MN/m^2; SE = 0.49; 15 cells analyzed) at $P \leq 0.05$ by the Wilcoxon test (Lapin, 1973). The loss modulus of control cells (1.13 MN/m^2; SE = 0.13; n = 17) also differs significantly from that of enzyme-treated cells (0.18 MN/m^2; SE = 0.11; n = 15) at $P \leq 0.01$ by the Wilcoxon test (Lapin, 1973).

These data and Eqs. 9, 10, 12, and 15 permit calculation of energy storage and dissipation in m^3 of muscle during the final ~2% passive extension. Control muscle stores 309 J/m^3 under these loading conditions while enzyme-treated muscle stores ~40% less (179 J/m^3). Even though control muscle stores more elastic energy, it is also far more energy dissipative. Approximately 993 J/m^3 are dissipated in control muscle while 226 J/m^3 are dissipated in enzyme-treated muscle. Specific losses in control muscle are nearly three times greater than in enzyme-treated muscle (1.6 vs. 0.6).

DISCUSSION

The mechanical role of skeletal muscle basement membranes has been investigated in the present study by

TABLE I
MECHANICAL BEHAVIOR OF CONTROL AND BASEMENT MEMBRANE–DEPLETED SKELETAL MUSCLE CELLS

Preparation	Complex modulus	Storage modulus	Loss modulus	Phase lag	Loss tangent	Energy stored	Energy dissipated	Specific loss
	MN/m^2	MN/m^2	MN/m^2	degrees		J/m^3	J/m^3	
Control cells*	3.29 (0.40)[‖]	3.09 (0.53)	1.13 (0.13)	20 (4.7)	0.37	309	993	1.6
Basement membranes‡ depleted cells	1.80 (0.28)	1.79 (0.49)	0.18 (0.11)	5.7 (3.2)	0.10	179	226	0.6
Basement membranes§	161	146	68.4	15.3	0.27	1.46×10^4	8.6×10^4	2.9

Measurement of complex modulus, phase lag, and loss tangent of control and enzyme-treated skeletal muscle cells. Cells at L_s = 2.6–2.8 μm were sinusoidally strained 0.7–2.7% at 1 Hz. Figures for energy input, returned and dissipated, are derived from the mean values of control and enzyme-treated cells for a 2% strain.

*17 cells analyzed.

‡15 cells analyzed.

§Calculated by difference between control cells and basement membrane depleted cells.

‖Numbers in brackets indicate standard errors.

comparing the mechanical behavior of intact skeletal muscle cells to cells from which basement membranes have been depleted. The interpretation of data from this investigation relies on the effectiveness and selectivity of the procedures used for basement membrane disruption. This discussion is directed, first, toward structurally and chemically defining basement membranes; second, toward appraising the basement membrane depletion technique used here; and, finally, toward discussing the mechanical behavior of basement membranes and the significance of these new findings.

Identification of Basement Membranes

Basement membranes were first identified as histological structures by light microscopy that permitted their localization subjacent to epithelia and around muscle fibers (Griepp and Robbins, 1983). In early histological studies, basement membranes could be distinguished from neighboring structures because they stained intensely with Schiff's reagent following periodic acid oxidation (PAS reaction). The PAS reaction indicates the presence of vicinal diglycols that are oxidized by periodic acid to form dialdehydes that may then react with the chromogen contained in the Schiff's reagent (Pearse, 1968).

PAS-positive substances are polysaccharides, glycoproteins, glycosaminoglycans, and glycolipids (Pearse, 1968) and include collagen (Pearse, 1968) and laminin (Timpl et al., 1979). Type IV collagen (Bornstein and Sage, 1980) and laminin (Timpl et al., 1979) comprise a major portion of basement membranes of all vertebrates studied thus far. These proteins may thereby account for much of basement membranes' PAS reactivity. Similarly, these same proteins bind WGA (Foidart et al., 1982) and may thereby comprise a major portion of the basement membranes' WGA-binding sites.

Electron microscopic studies of basement membranes from various tissues show similarities in the fine structure of each basement membrane. Basement membranes can be structurally subdivided into basal lamina and reticular lamina by ultrastructural appearance (Bernfield, 1984). The basal lamina is the layer lying closest to the supported cells and is the layer produced by those associated parenchymal cells. The reticular lamina lies external to this and is produced by connective tissue cells.

Thus, basement membranes can be defined by several criteria, including (*a*) morphologically according to histological location and electron microscopic appearance, (*b*) molecularly, as structures containing laminin and Type IV collagen, and (*c*) chemically, as cell surface structures that display lectin binding and PAS reactivity.

This definition of basement membrane pertains to all basement membranes studied so far. The definition differs from that of "sarcolemma," which is a term commonly used in discussions of muscle structure. Those who have previously studied the mechanical properties of "sarcolemma" (e.g., Ramsey and Street, 1940; Casella, 1951; Fields and Faber, 1970; Rapoport, 1973) use this term to refer to that portion of a muscle cell that remains intact after the cell is crushed and myofibrils retract to the ends of the fiber. The nonretracted portion of the fiber is thought to be comprised of basement membrane, plasma membrane, and possibly intracellular, plasma membrane-associated material.

Evaluation of Technique

Four experimental preparations have been used previously in studies of the mechanical behavior of muscle basement membrane or sarcolemma. These are the following: (*a*) skinned fibers from which the surface of the cell is stripped with needles or forceps (e.g., unpublished study cited by Magid and Law, 1985); (*b*) retraction clot studies, in which the cell is crushed and the myofibrils are allowed to retract away from the crushed region, thus leaving a sarcolemma tube (e.g., Ramsey and Street, 1940; Casella, 1951; Fields, 1970; Fields and Faber, 1970; Rapoport, 1973); (*c*) resting fibers, in which few actomyosin cross-bridges are present (e.g., Haugen and Sten-Knudsen, 1981); and (*d*) the elastimeter method, in which small

regions of sarcolemma are deformed with known forces by aspirating the cell's surface into a pipette using a known force and measuring deformation (Rapoport, 1972).

Each of the above experimental approaches is limited in effectiveness for studying the behavior of basement membrane. Skinned fibers are depleted of basement membrane, plasma membrane, and possibly subplasmalemmal structures, including components of the structural costameres that have been identified in striated muscle by Repasky et al. (1982) and Pardo et al. (1983). Furthermore, unknown and unintended structural damage may be incurred during skinning. Thus, resolution of the basement membrane's behavior is difficult. Retraction clot preparations involve unknown damage to sarcolemmal as well as myofibrillar elements. These preparations may also change the geometry of the cell that prohibits accurate stress and strain measurements. Resting fiber studies reduce the contribution of actomyosin to muscle stiffness, yet these preparations cannot resolve the relative contributions of sarcolemmal constituents and other, more recently discovered structural elements in muscle such as titin (e.g., Wang et al., 1979, 1984) and connectin (e.g., Maruyama et al., 1977, 1984, 1985).

The elastimeter method (Rapoport, 1972) may be superior to these other approaches in that the cell is not intentionally damaged before testing and the elements being loaded are more clearly defined. The elastimeter method may be limited, however, by the differences in the geometry of cell surface loading in which a bleb of membrane is drawn into a pipette. This may cause differences in the shear and tensile components of membrane loading from actual in vivo loading patterns.

The present study attempts to avoid these limitations through (*a*) an enzymatic removal of extracellular materials, (*b*) loading cells in ways that simulate loading in vivo, and (*c*) through confirmation by electrophoretic, lectin-binding, and electron microscopic techniques that only cell surface and extracellular structures are removed by the enzymatic treatment. This approach leaves intracellular structural elements unperturbed and normal cell and loading geometry intact.

Enzymatic treatments have not always been reported to be effective in removing muscle basement membrane. Bacterial collagenase used alone (Boyde and Williams, 1968) has been found effective at removing connective tissue from muscle cells when the treated muscles were subsequently studied by scanning electron microscopy. Another investigation has shown that collagenase treatments can digest basement membrane associated with isolated sarcolemma preparations (Kono et al., 1964). However, a later study (Zacks et al., 1973) reported that hyaluronidase and collagenase used together were ineffective at altering the electron microscopic appearance of muscle basement membrane.

The present study indicates through electrophoretic, lectin-binding, and electron microscopic analyses that enzymatic treatment followed by dissection to obtain single cells is effective at basement membrane removal. Enzyme-treated cells showed reduction of ^{125}I-WGA-binding proteins and a reduction in proteins of molecular weights characteristic of connective tissue components. These cells also appeared depleted of basement membrane when studied by electron microscopy. Furthermore, the enzyme-treated muscles used for mechanical testing still propagated action potentials following enzyme treatment, they displayed no change in the relative molar ratio of major cytoskeletal components seen in SDS PAGE and appeared intact when viewed by electron microscopy at the end of mechanical testing. Together, these findings indicate that the enzymatic treatment and subsequent dissection successfully removes basement membrane and other extracellular structures while leaving a living, contractile, intact cell. No attempt has been made in this study to identify or locate the proteins that are depleted during enzymatic treatment. Antibodies to these proteins are being manufactured currently to pursue this study.

Mechanical Behavior of Basement Membranes

Most investigators who have attempted to evaluate the mechanical behavior of basement membranes in muscle have been concerned with the role of the basement membrane in determining passive stiffness in muscle. Some of the earliest investigators (Ramsey and Street, 1940) concluded that much of the passive stiffness of muscle cells was attributable to the "sarcolemma." Here, the term "sarcolemma" refers to the plasma membrane and basement membrane. Subsequent work indicated that the sarcolemma became important in contributing to cell stiffness only after a cell was stretched ~50% longer than its rest length (Casella, 1951; Rapoport, 1973).

A more recent report (Magid and Law, 1985) concludes that the basement membrane and other connective tissue around muscle are functionally unimportant in determining stiffness until muscle is stretched beyond overlap of thin and thick filaments. However, this study is difficult to interpret in that highly nonphysiological strain rates were used and the conclusion relies upon comparisons to data not in the literature. Furthermore, the interpretation of data by these investigators (Magid and Law, 1985) relied upon the assertion that frog semitendinosus muscle doubles in length under physiological conditions. Other investigations have shown that muscles rarely shorten by >30% (Gans and Bock, 1965) and single sarcomeres can be reversibly contracted by no more than 40% (Rice, 1973). A subsequent study, in which sarcomere lengths of frog semitendinosus was measured at the points of maximum excursion of the limb during swimming, indicates that semitendinosus undergoes a maximum strain of ~24% during swimming (Tidball and Daniel, 1986).

The present study differs from others cited above, in which passive stiffness of the sarcolemma was investigated,

in that dynamic loading at physiological strains is used. Biological materials, such as the basement membrane, display time-dependent behavior when loaded; that is, their stiffness and energy storage capabilities vary with the rate and duration of loading. Investigations of passive stiffness commonly use applied loads of nonphysiological and occasionally unreported duration. Although such studies do give records of stiffness, the measurements may vary from physiological values.

Cells loaded in this study were strained ~2% at 1 Hz. An earlier study showed that in fast swimming, frog semitendinosus is strained ~20% at 1 Hz (Tidball and Daniel, 1986). The strain rate used in this study is therefore about one-tenth the strain rate experienced by the muscle in fast locomotion. However, there is no significant difference in stiffness of muscle in rigor or energy losses in sinusoidal loading between loading rates of 1 and 10 Hz (Kawai and Brandt, 1980).

Plotting stress versus strain for a single cycle of loading produces a Lissajous figure that graphically represents many features of the dynamic behavior of single cells during sinusoidal loading. Figure 6 shows the Lissajous figures obtained by loading a control cell and an enzyme-treated cell. The complex moduli of the cells in this figure are proportional to the slopes of the long axis of the two elliptical Lissajous figures. Note that the slope of the axis of the control cell and, therefore, its stiffness, is only slightly greater than that of the enzyme-treated cell. This stiffness data alone would suggest that the basement membrane's role in the mechanical behavior of these cells was small. However, the area enclosed within these Lissajous figures increases as the energy dissipation within the cell increases during loading (Buchthal and Kaiser, 1951). The Lissajous figures of these two cells, therefore, show that while there is little difference in the cells' stiffnesses, there are large differences in the efficiency of energy storage in intact cells versus cells without basement membranes. Through Eq. 16, the specific loss of energy during loading can be expressed for each preparation. The specific loss for control cells is nearly three times greater than in enzyme-treated cells.

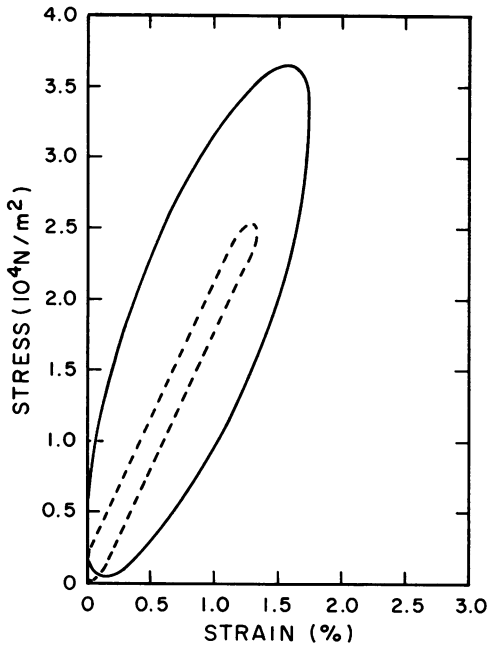

FIGURE 6 Lissajous figures of a control cell and enzyme-treated cell. The control cell (*solid line*) had E^* = 2.28 MN/m^2, tan δ = 0.27, E' = 2.20 MN/m^2, E'' = 0.60 MN/m^2 at ϵ = 1.7% and L_s = 2.7 μm. The enzyme-treated cell (*dotted line*) had E^* = 1.8 MN/m^2, tan δ = 0.09, E' = 1.79 MN/m^2, E'' = 0.16 MN/m^2 at ϵ = 1.4% and L_2 = 2.6 μm. The oscilloscope traces for both cells followed a clockwise direction through the cycle of loading, thus for each preparation more energy was put into the cell than was returned.

Calculations of the mechanical properties of basement membrane depend on the cross-sectional area of the loaded basement membrane. The range of thickness for basement membranes of single, dissected cells used in this study was 100–300 nm. The value used for sarcolemma thickness in previous investigations has been 100 nm (e.g., Fields and Faber, 1970; Rapoport, 1972, 1973). These investigations by Fields and Faber (1970) and Rapoport (1972, 1973) relied on measurements of sarcolemma thickness made in previous investigations in which (*a*) the investigator was attempting to measure the thickness of plasma membrane of a muscle of unstated origin (Barer, 1948); (*b*) the investigators used pieces of fixed or unfixed muscle that were air dried and viewed without sectioning through the electron microscope to measure sarcolemma thickness (Jones and Barer, 1948); (*c*) measurements were made of sarcolemma thickness of fixed, embedded, whole tissue from frog tibialis anticus (Mauro and Adams, 1961); (*d*) measurements of thickness of membranes and their surface coats were made from electron micrographs of partially purified sarcolemma preparations (McCollister, 1962); or (*e*) measurements of sarcolemma thickness were made microscopically from cooked beef blended in a Waring blender (Wang, 1956).

The present study, therefore, differs from previous studies of basement membrane mechanical behavior in that basement membrane thickness is measured electron microscopically in thin sections of the same cells that were prepared for mechanical testing. The range of basement membrane thicknesses measured in the present study (100–300 nm) reflects differences in the preparations obtained by mechanical dissection. The following calculations of the mechanical properties of skeletal muscle basement membrane use the median thickness of 200 μm. Since the basement membrane varies in thickness between single, dissected cells and varies in thickness along the length of any single cell, and since electron micrographs show that it is not a homogeneous material, attempts to determine more accurately the thickness of basement membranes in these preparations is not meaningful.

If the greater energy dissipation of control muscles versus enzyme-treated muscles is attributable to energy

losses that occur in the basement membrane, many of the mechanical properties of the basement membrane can be calculated. This difference in energy loss between the two preparations (767 J/m^3 of muscle) can be expressed in terms of energy losses per unit mass of basement membrane, assuming similar densities for muscle and basement membrane. The relative volume of a typical skeletal muscle cell which is 100 μm in diameter to an ensheathing basement membrane 200 μm thick is 112:1. Thus, energy loss (ξ_d) in the basement membrane during this stage of locomotion is 8.6×10^4 J/m^3 of basement membrane. Similarly, by assuming that the difference in energy stored in control cells (309 J/m^3) and enzyme-treated cells (179 J/m^3) is stored in basement membrane, and by correcting for the volume ratio of cell to basement membrane (112:1), the energy stored per unit volume of basement membrane can be calculated (1.46×10^4 J/m^3).

These values for E_d and E_s of basement membrane permit calculation of E' and E'' for basement membrane for ~2% strains through Eqs. 12 and 15. The value for tan $\delta(=E''/E')$ can then be calculated. Tan δ is then used to calculate the complex modulus, E^*, for basement membrane through either Eq. 9 or 10. These values are tabulated along with those of control and enzyme-treated muscle in Table I.

This value of E^* (161 MN/m^2) of skeletal muscle basement membrane is less than 10% of the value obtained for stiffness of sarcolemma in some static experiments (~2 GN/m^2; Fields and Faber, 1970). Possible reasons for this discrepancy may be that these earlier investigators assumed a sarcolemma thickness of 100 nm, they performed their measurements at unknown sarcomere lengths and used mechanically damaged fibers that had produced retraction clots.

Other investigators have produced much lower values for sarcolemma stiffness in static loading tests. Rapoport (1973) found that sarcolemma stiffness was ~6 MN/m^2 along the length of the fiber in retraction clot preparations and ~0.5 MN/m^2 in elastimeter method loading (Rapoport, 1972). Although Rapoport used 100 nm as an estimate of sarcolemma thickness in each of these studies, that thickness, which is smaller than the value used for basement membrane in the present study, should reduce the difference between Rapoport's values for stiffness and the values determined in the present study. The lower values for stiffness produced in Rapoport's studies than in the present study may result from differences in experimental approach. Rapoport loaded his test preparations and waited 10–15 min before recording tension. This delay in recording tension allowed stress in the preparation to decline as plastic deformations occurred in the cell. The continuously monitored stress and strain recorded in the study reported here reduced the magnitude of creep in the cell during recording that would thereby increase values for stiffness when compared to Rapoport's experimental approach.

The findings of the present study indicate that the mechanical behavior of skeletal muscle basement membrane influences the mechanical behavior of intact muscle in two ways. One significant mechanical feature is its contribution to elastic energy storage in muscle, as previously postulated (Tidball and Daniel, 1986). However, this study also shows that basement membranes function as elements that increase energy dissipation in muscle as the muscle reaches those lengths where passive extension ends and active contraction begins. This energy dissipated in the basement membrane exceeds the amount of energy stored in the basement membrane, as indicated by the greater specific loss of intact cells over basement membrane–depleted cells. This finding is potentially interesting with regard to whole muscle function, in that the basement membrane may help slow the passive extension of muscle immediately before active contraction during locomotion by dissipating energy at that stage. Thus, the basement membrane may act as a brake.

A morphological basis for the mechanism of energy dissipation is found in earlier studies (Schmalbruch, 1974; Tidball and Daniel, 1986), which note that at the sarcomere lengths considered here (L_s = 2.6–2.8 μm), fibrils at the cell surface are passively reoriented from oblique angles to the long axis of the cell to more nearly parallel to the cell. This reorientation may require energy that is not returned during active contraction.

The findings presented here and their interpretation pertain only to cells in rigor strained ~2% at L_s = 2.6–2.8 μm. This simulates cell length, strain, and crossbridge status at the stage in which the cell becomes active, is then stretched an additional ~2%, and then begins shortening. These skeletal muscle cells and their basement membranes are also strained ~20% during passive extension in locomotion while the cell is relaxed (Tidball and Daniel, 1986). The energy storing and dissipating role of the basement membrane during this earlier stage of passive extension has not yet been investigated.

The author thanks Ms. Michelle Gadus for skillful technical assistance and the referees of the *Biophysical Journal* for valuable critiques.

This work was supported by a Grant-in-Aid from the American Heart Association, California Affiliate and Ventura County Chapter. Additional support was received through National Science Foundation Grant DCB-8417485 and an Academic Senate of the University of California grant.

Received for publication 18 February 1986 and in final form 13 August 1986.

REFERENCES

Allen, R. C., C. A. Saravis, and H. R. Maurer. 1984. Gel Electrophoresis and Isoelectric Focusing. deGruyter, Berlin, New York. 184 pp.

Asmussen, E., and F. Bonde-Petersen. 1974. Storage of elastic energy in skeletal muscles in man. *Acta Physiol. Scand.* 91:385–392.

Barer, R. 1948. The structure of the striated muscle fibre. *Biol. Rev.* 23:159–200.

Bernfield, M. 1984. Introduction. *In* Basement Membranes and Cell

Movement. R. Porter and J. Whelan, editors. Ciba Foundation Symposium. 108:1–5.

Bernfield, M. R., and S. D. Bannerjee. 1978. The basal lamina in epithelial-mesenchymal morphogenetic interactions. *In* Biology and Chemistry of Basement Membranes, N. A. Kefalides, editor. Academic Press, Inc., New York, London. pp. 137–148.

Bornstein, P., and H. Sage. 1980. Structurally distinct collagen types. *Annu. Rev. Biochem.* 49:957–1003.

Boyde, A., and J. C. P. Williams. 1968. Surface morphology of frog striated muscle as prepared for and examined in the scanning electron microscope. *J. Physiol. (Lond.).* 197:10P–11P.

Brady, A. J., S. T. Tan, and N. V. Ricchiuti. 1979. Contractile force measured in unskinned isolated adult rat heart fibers. *Nature (Lond.).* 282:728–729.

Buchthal, F., and P. Rosenfalck. 1957. Elastic properties of striated muscle. *In* Tissue Elasticity. J. W. Remington, editor. American Physiological Society, Washington, D.C. 73–97.

Buchthal, F., and E. Kaiser. 1951. The rheology of cross-striated muscle fibers with particular reference to isotonic conditions. *Dan. Biol. Med.* 21:1–318.

Burnette, W. N. 1981. "Western Blotting": electrophoretic transfer of proteins from sodium dodecyl sulfate-polyacrylamide gels to unmodified nitrocellulose and radiographic detection with antibody and radioiodinated protein A. *Anal. Biochem.* 112:195–203.

Casella, C. 1951. Tensile force in total striated muscle, isolated fibre and sarcolemma. *Acta Physiol. Scand.* 21:380–401.

Cavagna, G. A., F. P. Saibene, and R. Margaria. 1965. Mechanical work in running. *J. Appl. Physiol.* 19:249–256.

Cavagna, G. A., N. C. Heglund and C. R. Taylor. 1977. Mechanical work in terrestrial locomotion: two basic mechanisms for minimizing energy expenditure. *Am. J. Physiol.* 233:R243–R261.

Farquhar, M. G. 1982. The glomerular basement membrane—a selective macromolecular filter. *In* The Cell Biology of the Extracellular Matrix. E. D. Hay, editor. Plenum Press, New York. 335–378.

Ferenczi, M. A., E. Homsher, D. R. Trentham, and A. G. Weeds. 1978. Preparation and characterization of frog muscle myosin subfragment 1 and actin. *Biochem. J.* 171:155–163.

Ferry, J. D. 1970. Viscoelastic Behavior of Polymers. 2nd edition. John Wiley, New York. 33–49, 570–572.

Fields, R. W. 1970. Mechanical properties of the frog sarcolemma. *Biophys. J.* 10:462–479.

Fields, R. W., and J. J. Faber. 1970. Biophysical analysis of the mechanical properties of the sarcolemma. *Can. J. Physiol. Pharmacol.* 48:394–404.

Foidart, J. M., R. Timpl, H. Furthmayer, and G. R. Martin. 1982. Laminin, a glycoprotein from basement membranes. *In* Immunochemistry of the Extracellular Matrix. H. Furthmayer, editor. CRC Press, Boca Raton, FL. 125–134.

Gans, C., and W. J. Bock. 1965. The functional significance of muscle architecture: A theoretical analysis. *Ergebnisse dur Anatomie und Entwicklungsgeschichte.* 35:115–142.

Griepp, E., and E. Robbins. 1983. Epithelium. *In* Histology: Cell Biology and Tissue Biology. L. Weiss, editor. Elsevier Publishing Co., New York. 109–137.

Haugen, P. and O. Sten-Knudsen. 1981. The dependence of short-range-elasticity on sarcomere length in resting isolated frog muscle fibres. *Acta Physiol. Scand.* 112:113–120.

Hay, E. D. 1978. Role of basement membranes in development and differentiation. *In* Biology and Chemistry of Basement Membranes. N. A. Kefalides, editor. Academic Press, Inc., New York, London. 119–136.

Hay, E. D. 1982. Cell-matrix interaction in embryonic avian cornea and lens. *In* Extracellular Matrix. S. Hawkes and J. L. Wang, editors. Academic Press, Inc., New York, London. 55–69.

Heathcote, J. G., and M. E. Grant. 1981. The molecular organization of basement membranes. *Int. Rev. Conn. Tiss. Res.* 9:191–264.

Hunter, W. M., and F. C. Greenwood. 1962. Preparation of iodine-131 labelled human growth hormone of high specific activity. *Nature (Lond.).* 194:495–496.

Jones, W. M., and R. Barer. 1948. Electron microscopy of the sarcolemma. *Nature (Lond.).* 161:1012.

Kawai, M., and P. W. Brandt. 1980. Sinusoidal analysis: A high resolution method for correlating biochemical reactions with physiological processes in activated skeletal muscles of rabbit, frog and crayfish. *J. Muscle Res. Cell Motil.* 1:279–303.

Kefalides, N. A., R. Alper, and C. C. Clark. 1979. Biochemistry and metabolism of basement membranes. *Int. Rev. Cytol.* 61:167–228.

Kono, T., F. Kakuma, M. Homma, and S. Fukuda. 1964. The electron-microscopic structure and chemical composition of the isolated sarcolemma of the rat skeletal muscle cell. *Biochim. Biophys. Acta.* 88:155–176.

Laemmli, U. K. 1970. Cleavage of structural proteins during the assembly of the head of bacteriophage T_4. *Nature (Lond.).* 227:680–685.

Lapin, L. L. 1973. Wilcoxon two-sample rank-sum test. *In* Statistics for Modern Business Decisions. Harcourt, Brace, Jovanovich, Inc., New York, Chicago. 407–414.

Magid, A., and M. K. Reedy. 1980. X-ray diffraction observations of chemically skinned frog skeletal muscle processed by an improved method. *Biophys. J.* 30:27–40.

Magid, A., and D. J. Law. 1985. Myofibrils bear most of the resting tension in frog skeletal muscle. *Science (Wash. DC).* 230:1280–1282.

Marsden, C. D., J. A. Obeso, and J. C. Rothwell. 1983. The function of the antagonist muscle during fast limb movements in man. *J. Physiol. (Lond.).* 335:1–13.

Maruyama, K., S. Matsubara, R. Natori, Y. Nonomura, S. Kimura, K. Ohashi, F. Murakami, S. Handa, and G. Eguchi. Connectin, an elastic protein of muscle. Characterization and function. *J. Biochem.* 82:317–337.

Maruyama, K., S. Kimura, H. Yoshidomi, H. Sawada, and M. Kikuchi. 1984. Molecular size and shape of β-connectin, an elastic protein of skeletal muscle. *J. Biochem.* 95:1423–1433.

Maruyama, K., T. Yoshioka, H. Higuchi, K. Ohashi, S. Kimura, and R. Natori. 1985. Connectin filaments link thick filaments and Z-lines in frog skeletal muscle as revealed by immunoelectron microscopy. *J. Cell Biol.* 101:2167–2172.

Mauro, A., and W. R. Adams. 1961. The structure of the sarcolemma of the frog skeletal muscle fiber. *J. Biophys. Biochem. Cytol.* 10:177–185.

McCollister, D. L. 1962. A method for isolated skeletal-muscle cell-membrane components. *Biochim. Biophys. Acta.* 57:427–437.

Mobley, B. A., and B. R. Eisenberg. 1975. Sizes of components in frog skeletal muscle measured by methods of stereology. *J. Gen Physiol.* 66:31–45.

Pardo, J. V., J. D. Siliciano, and S. W. Craig. 1983. A vinculin-containing cortical lattice in skeletal muscle: Transverse lattice elements ("costameres") mark sites of attachment between myofibrils and sarcolemma. *Proc. Natl. Acad. Sci. USA.* 80:1008–1012.

Pearse, A. G. E. 1968. Oxidation methods for mucosubstances. *In* Histochemistry: Theoretical and Applied. Vol. 1. Williams and Wilkins, Baltimore. 307–322.

Ramsey, R. W., and S. F. Street. 1940. The isometric length-tension diagram of isolated skeletal muscle fibres of the frog. *J. Cell Comp. Physiol.* 15:11–34.

Rapoport, S. I. 1972. Mechanical properties of the sarcolemma and myoplasm in frog muscle as a function of sarcomere length. *J. Gen. Physiol.* 59:559–585.

Rapoport, S. I. 1973. The anisotropic elastic properties of the sarcolemma of the frog semitendinosus muscle fiber. *Biophys. J.* 13:14–36.

Repasky, E. A., B. L. Granger, and E. Lazarides. 1982. Widespread occurrence of avian spectrin in non-erythroid cells. *Cell.* 29:821–833.

Rice, M. J. 1973. Supercontracting striated muscle in a vertebrate. *Nature (Lond.).* 243:238–240.

Sanders, E. J. 1983. Recent progress towards understanding the roles of

the basement membrane during development. *Can. J. Biochem. Cell. Biol.* 61:949–956.

Schmalbruch, H. 1974. The sarcolemma of skeletal muscle fibres as demonstrated by a replica technique. *Cell Tiss. Res.* 150:377–387.

Tidball, J. G. 1983. The geometry of actin filament-membrane associations can modify adhesive strength of the myotendinous junction. *Cell Motil.* 3:439–447.

Tidball, J. G., and T. L. Daniel. 1986. Elastic energy storage in rigored skeletal muscle cells under physiological loading conditions. *Am. J. Physiol.* 250:R56–R64.

Timpl, R. H., H. Rohde, P. Gehron Robey, S. I. Rennard, J. M. Foidart, and G. R. Martin. 1979. Laminin: a glycoprotein from basement membranes. *J. Biol. Chem.* 254:9933–9937.

Van Exan, R. J., and B. K. Hall. 1983. Epithelial induction of osteogenesis in embryonic chick mandibular mesenchyme: a possible role for basal lamina. *Can. J. Biochem. Cell. Biol.* 61:937–979.

Wang, H. 1956. The sarcolemma and fibrous envelope of striated muscles in beef. *Exp. Cell Res.* 11:452–463.

Wang, K., J. McClure, and A. Tu. 1979. Titin: major myofibrillar components of striated muscle. *Proc. Natl. Acad. Sci. USA.* 76:3698–3702.

Wang, K., R. Ramirez-Mitchell, and D. Patter. 1984. Titin is an extraordinarily long, flexible and slender myofibrillar protein. *Proc. Natl. Acad. Sci. USA.* 81:3686–3689.

Zacks, S. I., M. F. Sheff, and A. Saito. 1973. Structure and staining characteristics of myofiber external lamina. *J. Histochem. Cytochem.* 21:703–714.